Available online at www.sciencedirect.com
ScienceDirect
Biochimica et Biophysica Acta 1768 (2007) 253–263
Biochimica et Biophysica Acta BBA
www.elsevier.com/locate/bbamem

The properties of *Bacillus cereus* hemolysin II pores depend on environmental conditions

Zhanna I. Andreeva [a], Vladimir F. Nesterenko [a], Maria G. Fomkina [b], Vadim I. Ternovsky [c], Natalia E. Suzina [a], Anastasia Yu Bakulina [d], Alexander S. Solonin [a], Elena V. Sineva [a,*]

[a] *Institute of Biochemistry and Physiology of Microorganisms, Russian Academy of Sciences, Pushchino, Moscow Region, 142290, Russia*
[b] *Institute of Theoretical and Experimental Biophysics, Russian Academy of Sciences, Moscow Region, Pushchino, 142290, Russia*
[c] *Institute of Cell Biophysics, Russian Academy of Sciences, Moscow Region, Pushchino, 142290, Russia*
[d] *State Research Center of Virology and Biotechnology "VECTOR", Koltsovo, Novosibirsk Region, 630559, Russia*

Received 5 June 2006; received in revised form 3 November 2006; accepted 3 November 2006
Available online 10 November 2006

Abstract

Hemolysin II (HlyII), one of several cytolytic proteins encoded by the opportunistic human pathogen *Bacillus cereus*, is a member of the family of oligomeric β-barrel pore-forming toxins. This work has studied the pore-forming properties of HlyII using a number of biochemical and biophysical approaches. According to electron microscopy, HlyII protein interacts with liposomes to form ordered heptamer-like macromolecular assemblies with an inner pore diameter of 1.5–2 nm and an outer diameter of 6–8 nm. This is consistent with inner pore diameter obtained from osmotic protection assay. According to the 3D model obtained, seven HlyII monomers might form a pore, the outer size of which has been estimated to be slightly larger than by the other method, with an inner diameter changing from 1 to 4 nm along the channel length. The hemolysis rate has been found to be temperature-dependent, with an explicit lag at lower temperatures. Temperature jump experiments have indicated the pore structures formed at 37 °C and 4 °C to be different. The channels formed by HlyII are anion-selective in lipid bilayers and show a rising conductance as the salt concentration increases. The results presented show for the first time that at high salt concentration HlyII pores demonstrate voltage-induced gating observed at low negative potentials. Taken together we have found that the membrane-binding properties of hemolysin II as well as the properties of its pores strongly depend on environmental conditions. The study of the properties together with structural modeling allows a better understanding of channel functioning.

Keywords: *Bacillus cereus*; Pathogenicity; Pore-forming toxin; Hemolysin; Cytolysin

1. Introduction

Bacillus cereus is an opportunistic human pathogen well known as a food pollutant and contaminant of cosmetics and found to be a causative agent of endophthalmitis, food poisoning and wound infections [1,2]. The closely related microorganisms of the *B. cereus* group (*B. cereus, B. thuriengiensis* and *B. anthracis*) produce a wide range of toxins and demonstrate distinct pathogenic properties. For instance, *B. anthracis* is an agent of anthrax, a deadly disease of man and animals. *B. thuringiensis* is pathogenic to insects, and its extensive use as insecticide leads to uncontrollable proliferation of the microorganism in ecosystems. The mechanisms, including pathogenicity, that make these bacteria so adaptive to different ecological niches are not fully understood. Studies of the factors and means that allow bacteria to survive in warm-blooded organisms are extremely important for proper

Abbreviations: αHL, α-hemolysin of *Staphylococcus aureus*; HlyII, hemolysin II of *Bacillus cereus*; RBC, red blood cells; HU, hemolytic unit; βPFT, β-barrel pore-forming toxin; PMSF, phenylmethylsulfonylfluoride; PEG, polyethylene glycol

* Corresponding author. Current address: Pennsylvania State University, 307 South Frear, University Park, PA 16802, USA.
E-mail addresses: solonin@ibpm.pushchino.ru (A.S. Solonin), esineva@gmail.com (E.V. Sineva).

0005-2736/$ - see front matter © 2006 Elsevier B.V. All rights reserved.
doi:10.1016/j.bbamem.2006.11.004

estimation of environmental risks and prediction of emergent diseases [3].

One of several cytolytic proteins produced by *B. cereus* is hemolysin II (HlyII) [4,5]. Based on its deduced amino acid sequence, HlyII is a member of the family of oligomeric β-barrel pore-forming toxins (βPFT) [6,7]. This family also includes a number of *Staphylococcus aureus* cytolysins (α-toxin, leukocidins, γ-hemolysin) [8,9], *Clostridium perfringens* β-toxin [10] and *B. cereus* CytK toxin [11]. These toxins are secreted in a soluble form and cause their cytolytic effect by assembling into a transmembrane pore. The most studied representative of the family, α-toxin (αHL) of *S. aureus*, is the major cause of pathogenicity of this microorganism. Its biochemical and pore-forming properties studied in great detail are mediated by the formation of a heptameric channel of about 240 kDa. αHL monomers insert themselves into the cell membrane and oligomerize to form a wide transmembrane pore. The high resolution X-ray structure of the heptameric assembly was determined [12]. It is shaped like mushrooms of about 10 nm in height and diameter. The size of the pore ranges from 1.5 to 4.6 nm. Its channel is weakly anion-selective. A wealth of biochemical and electrophysiological data available about *S. aureus* αHL led to the detailed understanding of the pathogenic properties of the microorganism. For example, the absence of α-toxin or its inactivation leads to the disturbance of biofilm formation by *S. aureus*, which is an important factor of recurrent or chronic staphylococcal infections [13]. Thus, studies of the βPFT family are important in many aspects: (i) these toxins are involved in serious pathologies of man and farmed animals, (ii) they are a good model system to investigate protein–membrane interactions and (iii) they are the basic elements for the construction of nanopores for biotechnological applications in various fields [14,15].

Earlier, we demonstrated that cloning of *hlyII* gene from *B. cereus* conferred a hemolytic activity on *E. coli* cells [4]. Surprisingly, *hlyII* gene was found to be more widespread in *B. thuriengiensis* strains than in *B. cereus* [5]. Recently, we reported that a product of another gene, *hlyIIR*, located immediately downstream of *hlyII*, was a transcriptional regulator that interacted with the operator region of hemolysin gene [16]. Preliminary characterization of HlyII was done using very limited quantities of the protein obtained in a cell-free expression system [7]. Recently, we published a procedure for the purification of hemolysin II from bacterial culture and explored its cytotoxic properties [17]. The present article investigated interactions of hemolysin II with membrane and the properties of its pores. Several biochemical and biophysical methods were used to study this process, and we also performed a 3D modeling of the pore structure. The environmental conditions strongly influenced the properties of HlyII pores to lead to heterogeneity of the channels formed and to result in a complex electrophysiological behavior. It raises some important questions about the mechanisms of pore assembling and functioning in model and natural systems.

2. Materials and methods

2.1. Molecular modeling and alignments

Protein homology modeling is a computational technique based on the fact that a tertiary 3D structure is more conserved than a protein sequence [18]. In order to make models of HlyII, we used MUSCLE [19] for multiple alignments of all homological sequences found by BLAST [20] and determined highly conserved residues. The 3D structure of α-hemolysin from *S. aureus* (7AHL) is the only appropriate template for homology modeling of HlyII heptamer found in the PDB databank [12]. 94 residues of C-term of HlyII are absent in 7AHL and cannot be modeled using the direct homology modeling approach. Several alternative alignments of HlyII without C-term *vs*. 7AHL were made. Frankenstein server (http://genesilico.pl/frankenstein/) was used to generate an optimal model of heptamer taking into account highly conserved residues. Finally, the quality check of the predicted structure was performed using Verify3D [21] program to ensure its satisfactory quality.

2.2. Purification of HlyII from the culture supernatant

Hemolysin II protein as soluble monomer was purified from the culture of *E. coli* Z85 (pUJ2) cells [4] by a combination of ion exchange, affinity chromatography and gel-filtration as described [17]. The purified protein was stored at −20 °C. The quantitative hemolysis assay was described previously [4,17,22]. For hemolysin II solutions, 1 hemolytic unit (HU) per ml corresponds to the concentration of 2 ng/ml (50 pM).

2.3. Osmotic protection assay

The assay is based on the inhibitory effect of osmotic protectants on HlyII-induced hemolysis. The 1% erythrocyte suspension was mixed with an equal volume of hemolysin (10 HU/ml) in PBS in the presence of osmotic protectants, 30 mM PEGs of different molecular weights. The osmotic protectants were assumed to have the following hydrodynamic diffusion radii: PEG 200, 0.56 nm; PEG 400, 0.68 nm; PEG 600, 0.8 nm; PEG 1000, 1.0 nm; PEG 6000, 2.83 nm. The samples were incubated for 30 min, which was followed by precipitation of unlysed cells and determination of the optical density (545 nm) of the supernatants [6,23]. The normalized optical density of hemoglobin released from erythrocytes was plotted against the average hydrodynamic radii of PEGs.

2.4. Temperature jump experiments

1 HU of HlyII was incubated with a 0.5% erythrocyte suspension in the presence of 30 mM PEGs 600 and 1000 at either 4, 25 or 37 °C. PEG was removed from the erythrocytes by centrifugation, which was followed by a brief wash (1 min total time) of the cells with ice-cold PBS. Each sample was divided, and incubation was continued for another 30 min at 25 °C. The release of hemoglobin was scored as usual.

2.5. Electron microscopy of HlyII oligomers formed on liposomes

To prepare the liposomes, a 1 mg/ml lecithin solution in the mixture of chloroform and methanol (molar ratio, 2:1) was used. After drying under vacuum, the lipid film was resuspended in buffer (10 mM Tris–HCl, pH 7.2, 100 mM KCl) to a total lipid concentration of 1 mg/ml. Liposomes were prepared by ultrasonication for 30 min on ice using an ultrasonic disintegrator. 100 μl HlyII (30 μg/ml) was incubated with 20 μl freshly prepared liposomes at room temperature. The samples were adsorbed on formvar-coated copper grids and negatively stained with 0.5% (w/v) uranyl acetate. Micrographs were recorded at a nominal magnification of 80,000× on a JEM-100B (JEOL) electron microscope operating at 80 kV.

2.6. Planar bilayer lipid membrane recordings

Planar lipid bilayer membranes (BLM) were formed from soybean L-α-phosphatidylcholine (Type IV-S) dissolved in *n*-heptane (20 mg/ml) on a

0.4 mm-diameter aperture in a two-chamber teflon cell. The *cis* and *trans* chambers containing KCl buffer solution (1 ml each) were separated by the BLM deposited by the Mueller technique [24]. Various concentrations of KCl in 5 mM HEPES–KOH, pH 7.4 were used. Experiments were carried out under voltage-clamp conditions. The *trans* compartment was connected to the virtual ground through a Keithley 301 operational amplifier in a current-to-voltage configuration. The experiment was monitored by a PC connected to DT2801A (Data Translation, USA) or L-card 154 (L-card, Russia) AD-DA converters. The membrane potential was maintained using Ag/AgCl electrodes in 3 M KCl, and 2% agarose bridges. Data were recorded using BLM software developed by Dr. Anatoly Ya. Silberstein. Single channel conductance was determined by fitting peaks of amplitude histograms to Gaussian functions. Numerical values are given as means±SD. The experimental results were analyzed in Origin 7 and SigmaPlot 8. The current–voltage (I–V) characteristics for single channels were determined by subjecting the membrane to stepwise voltage changes and recording the resulting current. For ion selectivity measurements, different concentrations of KCl solutions were placed in *cis* (1 M KCl) and *trans* chambers creating a concentration gradient. After addition of the toxin, the reversal potential (V_{rev}) was experimentally determined and the permeability ratio (P_K^+/P_{Cl}^-) was calculated by using the Goldman–Hodgkin–Katz equation for monovalent ions [25] along with appropriate activity coefficients for KCl solutions.

$$P^+/P^- = [([a]_t/[a]_c)\exp(eV_{rev}/kT) - 1]/[([a]_t/[a]_c) - \exp(eV_{rev}/kT)] \quad (1)$$

where $[a]_c$ and $[a]_t$ are the KCl activities in the *cis* and *trans* solutions, respectively, e is the elementary charge, k and T have their usual meaning (kT/e is ≅ 25 mV at room temperature). HlyII protein was added to the *trans*-compartment to a final concentration of 2 nM. All measurements were made at room temperature (25±3 °C).

3. Results

3.1. Protein alignments and 3D modeling

Homology modeling is usually the method of choice when there is a strong similarity between the sequence of target protein and at least one known 3D structure. The choice of template is dictated by the availability of appropriative crystal structure. The HlyII protein sequence (excluding 94 C-terminal amino acids) has a sufficient similarity with the sequence of *S. aureus* α-hemolysin for homology modeling (31% identity, 60% positives) (Supplement, Figs. 1 and 2). The crystal structure (1.9 Å) of αHL pore [12] formed by seven identical subunits has been used to build a model of HlyII pore. The RMS distance between C_α-atoms of the modeled HlyII and staphylococcal αHL structure varied by 0.5–0.8 Å, depending on the method of measurements (e.g. the set of atoms to compare). The modeled heptameric complex of HlyII has a mushroom shape and comprises the cap domain, stem domain and seven rim domains (Fig. 1A). The oligomer measures about 10 nm in diameter, 10 nm in height, and the pore diameter varies from 1 to 4 nm along the channel length. The diameter of the heptameric HlyII pore is around 2 nm at the entrance, has a maximum of 4 nm inside the cap, 1.2 nm at the base of the transmembrane stem and 1 to 1.6 nm along the rest of the stem (Fig. 1B and C). The narrowest diameters highly depend on the positions of the long side chains of the charged residues inside the pore and, as result, can vary under different conditions and dramatically influence the pore properties.

It is a known fact that homology models are usually closer to templates than to native structures [18], but it is worth comparing the α-hemolysin and HlyII structures in an attempt to explain the difference in their properties. First, the stem region of HlyII is slightly longer (3 aa) and contains more charged amino acid groups. In contrast to α-hemolysin, there are no solvent-exposed hydrophobic residues on the interior surface of the pore. There are two belts of charged residues inside the stem domain of α-hemolysin: one is formed with E111 and K147 at the top of the stem and the other is D127, D128 and K131 at the stem base, without any charged residues in between (besides the partially charged H144). The distribution of charges in the HlyII interior is completely different, we can see four charged belts: K105 and D146 (at the top of the stem); E109 and K140; K119 and D130; D124 and K125 (at the stem base) (Fig. 1D and E). Approximate distances between C_α atoms of the belts are 1.3, 2.5 and 1.5 nm (Fig. 1C). Also, αHL has seven small side holes in the stem, which are surrounded by H144 residues. The holes allow a small molecule exchange between the interior and bulk solution; the protonation of H144 residues seems to affect the ion conductance, suggesting that the histidine ring can be the pH sensor that gates the conductance of αHL [26]. The corresponding residue in the HlyII structure is quite different, E141 (Fig. 1B). The small hole in the channel walls can be found in the model structure near this glutamate residue. It would be interesting to check whether this residue could affect the conductance of HlyII pores (Supplement, Fig. 3).

Surprisingly, residues suggested to be involved in protomer–protomer interactions are not conserved well in the primary protein structures of two hemolysins. Probably, predominantly the backbone–backbone type of interaction between the subunits in the pore, as well as the absence of strict geometric limitations for this type of interaction lead to the spreading of neutral amino-acid substitutions after gene divergence. In contrast, part of the HlyII rim domain (176–197, 250–259 aa), probably interacting with membrane [12], has the highest identity frequency with the template sequence (see Supplement, Fig. 2). The homology modeling of HlyII monomer using three leukocidin crystal structures as templates yielded very similar structure. The cartoon plotting the structures is given in Supplement (Fig. 4). Successful modeling of HlyII monomer using the structures of octameric cytolysins suggests that HlyII can also form octameric pores. To verify this possibility, we performed the modeling of HlyII octameric and hexameric caps using the M-ZDOCK program (http://zlab.bu.edu/m-zdock/). We found no steric hindrances that could prevent the formation of the channel with a larger number of subunits (e.g., octamer), but the formation of hexamer could be difficult because of long charged amino-acid side chains directed inside the channel ([27], Supplement, Fig. 5).

The success in the modeling of heptameric HlyII could not be considered as proof that heptamer is the only possible form of the pores, yet it can serve as an illustration of βPFT family common design and be a useful scientific tool to explain our experimental results in structural terms. Bearing in mind the results of *in silico* modeling [27] of different oligomeric forms, it is highly probable that heptamer is not the only possible form [28,29].

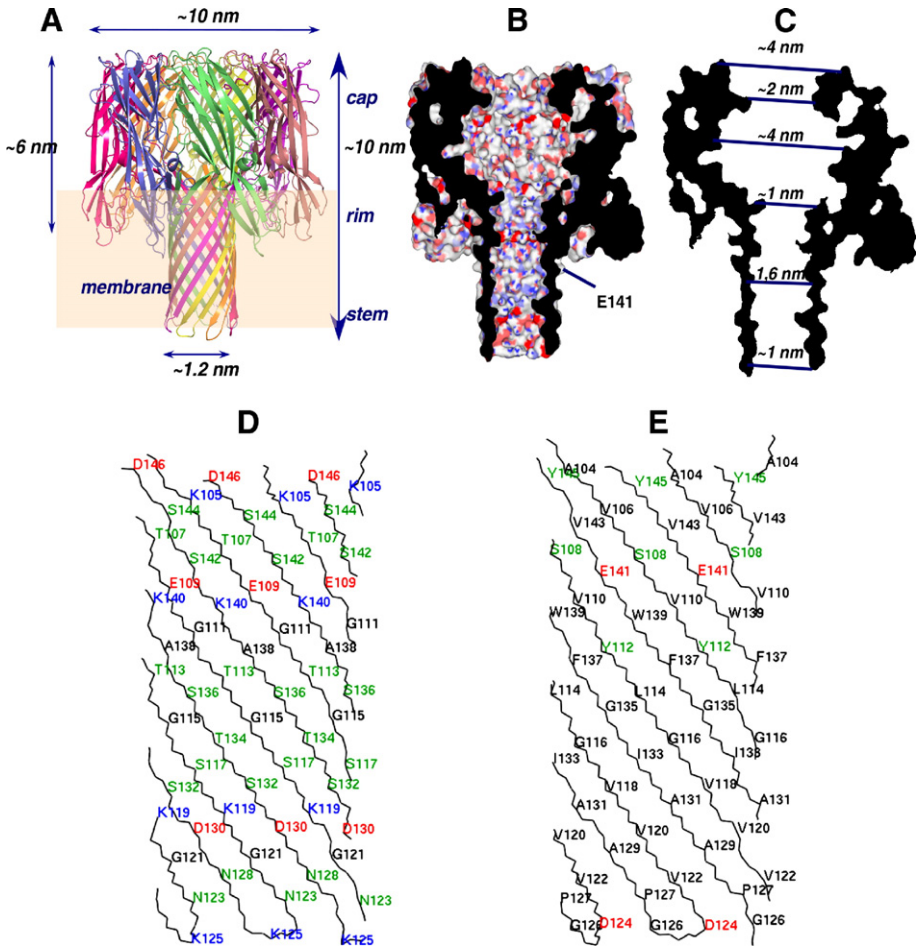

Fig. 1. Molecular models of the hemolysin II heptameric pore. Molecular modeling was performed using the 3D structure of αHL heptameric pore (7AHL, [9]) as described in Materials and methods. (A) Ribbon representation of the heptameric HlyII pore inserted in lipid bilayer. The cartoon shows the relative sizes of the pore and the position of the channel stem in the lipid bilayer. (B, C) Longitudinal slit through the seven-fold axis of heptameric HlyII pore. The charged residues' surface inside the constriction is shown as red (negative) and blue (positive) (B). The approximate internal channel radii are shown (C). (D, E) Schematic representation of the residues-defined inner and outer surfaces of the HlyII stem domain. The α-carbons of the stem were projected onto the surface of a cylinder, which was then unrolled as described in [10]. Residues are color-coded: Ser, Thr, Asn and Tyr: light green; Asp, Glu: red; Lys, Arg: blue; the rest is black. In the left (D) and right (E) vertical strips, there are the residues whose side chains are projected to the interior and exterior of the channel, respectively. (For interpretation of the references to colour in this figure legend, the reader is referred to the web version of this article.)

3.2. HlyII protein pores have an entrance diameter of about 2 nm

Inhibition of cytolysis by osmotic protectants has been employed in many studies of pore-forming cytolysins [6,23,30]. A direct method of assessing the hydrodynamic radius of the pore formed by toxins on RBC membranes is based on the determination of the hemolysis rate in the presence of different-size neutral solutes, e.g., using a series of increasing-size PEGs.

Osmotic protection experiments were performed using a purified mature HlyII toxin and human erythrocytes both at 4 and 37 °C. The results were indistinguishable at both temperatures. The hemolytic activity was nearly unaffected by PEG 200 but a significant protection effect of about 40% was observed in the presence of PEG 400. No hemolysis was noticed when erythrocytes were incubated with HlyII in solutions of higher molecular-weight PEGs (600–6000). As expected, the relative permeability of the osmolytes was inversely related to their size. The data were arranged in a plot (see Fig. 2A), providing an estimate of pore radius. The HlyII activity was inhibited totally by osmotic protectants with average molecular diameters larger than 1.6 nm and partially by that of 1.4 nm. Colloids with diameters of 0.9 nm or smaller did not protect against the HlyII-induced hemolysis. These results suggest that hemolysin II acts as a pore-forming hemolysin with a functional diameter of pores of about 1.5 nm. The results of these experiments were not sensitive to the HlyII protein concentration in the range from 1 to 20 HU/ml.

Pore formation was observed by electron microscopy (Fig. 2B–G). The analysis of electron microphotographs of negatively stained lipid vesicles formed in the presence of HlyII revealed numerous stain-filled ring-shaped assemblies clustered together. Some pores were approximately circular in shape, although some of them were less ideal in appearance, which was probably due to the sample preparation procedure. The majority of these assemblies had an inner pore diameter of about 2 nm and an outer diameter of about 8 nm. These data taken together are consistent with pore size and shape obtained from the analysis of the HlyII

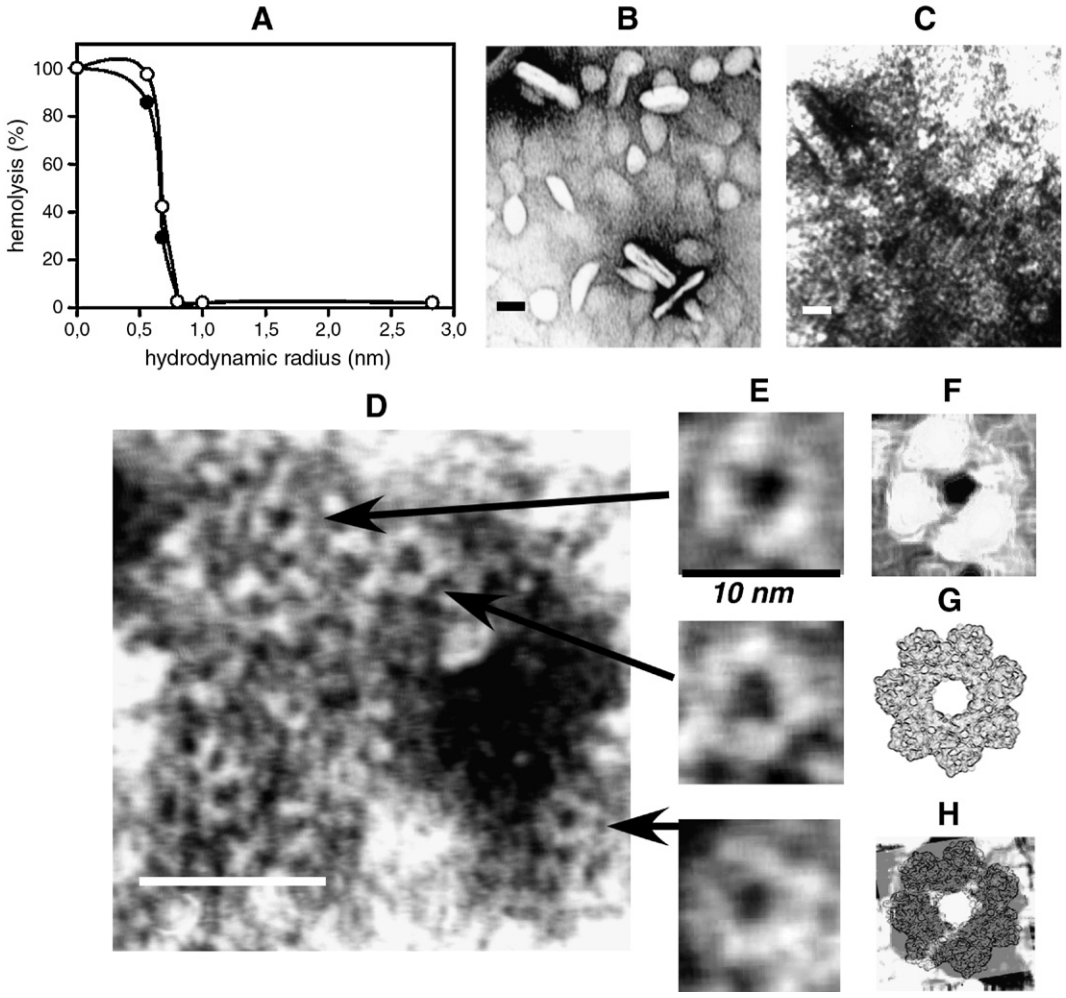

Fig. 2. Hemolysin II in lipid vesicles imaged by electron microscopy. (A) Inhibitory effect of osmotic protectants on HlyII-induced hemolysis. The final concentration of the protectants was 30 mM. The osmotic protectants were assumed to have the following hydrodynamic diffusion radii: PEG 200, 0.56 nm; PEG 400, 0.68 nm; PEG 600, 0.8 nm; PEG 1000, 1.0 nm; PEG 6000, 2.83 nm. The experiments were done at 4 °C (filled circles) and 37 °C (open circles). (B–E) The micrograph shows negatively stained vesicles containing HlyII. Scale bar (lower left) represents 200 Å. Liposomes (80,000×) (B). Liposomes with HlyII (80,000×) (C). Digital zoom image of C (D). Enlarged images of separate pores taken from image D (E). The arrows indicate pore locations. (F–H) Similarity between the computer model and EM results. Digitally treated image of HlyII pore (contrast and edge shaping) (F). Reconstruction of the pore top obtained from the results of 3D homology modeling (G). Digital overlap of images E and F to demonstrate the similarity between the computer model and EM results (H).

pore model (Fig. 2H). Based on the comparison of the EM images with the 3D model we believe that the diameter of the pore entrance is larger than the channel interior in the narrowest sites, as we observed on electron microphotographs and concluded from osmotic protection assays.

3.3. The first step of HlyII interaction with membranes does not depend on temperature

Analysis of the dose–response curves (Fig. 3A) demonstrated that at all temperatures tested, at the 30 min time point, the dependence of hemoglobin release on the HlyII concentration was steep and sigmoid. Higher concentrations of HlyII were required to obtain the same extent of hemolysis at 4 °C. The dose–response curves were smoother when the time point of 5 min was taken (Fig. 3B). During this time, the hemolysis was negligible at 4 °C. The steep mode of hemolysis suggests that the lysis was accompanied by cooperative events between the toxin molecules, thus confirming the oligomeric nature of HlyII pores and the fact that oligomerization is temperature-dependent. Based on these results as well as the inactivation kinetics of HlyII in solution (data not shown), we propose that HlyII binds to and, probably, interacts with the membrane as a monomer or an oligomer of a few subunits. Further oligomerization occurs when toxin molecules bind in close proximity to one another, and pores are formed from larger oligomers.

Then, we analyzed the kinetics of erythrocyte lysis by HlyII at temperatures from 4 to 37 °C (Fig. 3C and D). At high concentrations of hemolysin II (2 HU/ml), the hemolysis rate was identical both at 25 and 37 °C, with 100% hemolysis achieved in 20 min, without any significant lag in the lysis (Fig. 3C). There was a slight drop in the hemolysis rate at 15 °C, though 100% hemolysis was observed in 30 min. At 4 °C, the kinetics was rather different. Hemolysis started with at least a 10-min delay. A longer lag period at 4 °C suggests that the overall rate of pore formation is lower than that at higher

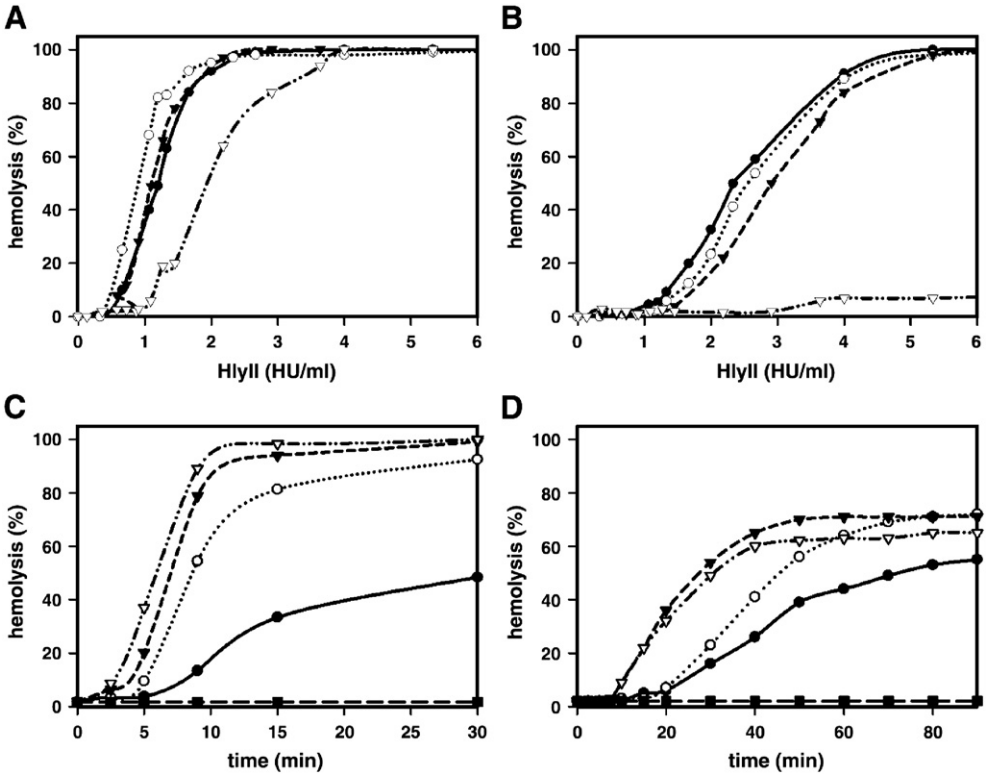

Fig. 3. The pore-forming properties of hemolysin II. (A, B) Hemolytic dose–response curves were taken at different temperatures. Serial HlyII dilutions (0–6.5 HU/ml final) were incubated with 1% suspension of human erythrocytes in PBS at 4 °C (open triangles), 15 °C (filled triangles), 25 °C (open circles) and 37 °C (filled circles) for 30 (A) and 5 min (B). The extent of hemolysis was monitored as described in Materials and methods. (C, D) Hemolytic activity of HlyII at different temperatures. Briefly, 30 HU and 15 HU of HlyII, (C and D panels, respectively) was added to 15 ml (final volume) of 1% (v/v) human erythrocytes in PBS, pre-heated at 4 °C (filled circles), 15 °C (open circles), 25 °C (filled triangles) and 37 °C (open triangles). The incubation continued at the pre-incubation temperatures. The extent of hemolysis of the samples was followed by measuring the absorbance of the released hemoglobin. The spontaneous hemolysis was nearly absent (filled squares). Each curve represents the average of three independent experiments. The error bars (not shown) were within the 5% limit of data values.

temperatures. In contrast, the rate of hemolysis after the lag period was less dependent on temperature. The kinetics of erythrocyte lysis at higher HlyII concentration 3.3 HU/ml can be seen in Fig. 6 in the Supplement. When a lower concentration of HlyII (Fig. 4D) was used in the same test (1 HU/ml), the lag period was about 10 min at any temperature tested. The lag was longer at 4 and 15 °C. A striking difference was observed when comparing the overall yield of hemolysis. Surprisingly, 37 °C was found to be not an optimal temperature; at 37 °C, the hemolysis was faster than at 15 °C, but the final yield under these conditions never reached the score of 25 °C. Both the overall rate and extent of hemolysis were lowest at 4 °C.

At least four possible steps in pore formation could be affected by low temperature: (i) membrane binding, (ii) conformational change during insertion, (iii) oligomerization or (iv) pore opening/closing [3]. To explore if the delay in lysis was due to the temperature dependence of HlyII binding to the erythrocyte membrane, we performed temperature jump experiments. HlyII (1 HU/ml) was incubated with erythrocytes at 4 °C, and samples were taken at certain time points (after 2.5, 5 and 10 min). During the incubation time, the extent of hemolysis was found to be negligible. Then, cells were washed twice with ice-cold PBS to remove unbound toxin and were transferred to the 37 °C routine. The hemoglobin release was compared with the samples incubated without washing during the same time at 37 °C. No significant differences between the tested and control samples were found after incubation for 20 min. Thus, the first step of HlyII binding to the cell membranes does not depend on temperature and occurs rapidly at any temperature. We demonstrated that HlyII could bind to the membrane during the lag period at 4 °C. Probably, at low temperatures the slowest step is pore opening.

3.4. HlyII pore structures formed at 4 °C and 37 °C differ

A mechanism of action was proposed according to which the toxin, HlyII, would be inserted into the membrane outer monolayer, thereby increasing the lateral tension as more monomers were cooperatively incorporated, up to membrane collapse and reorganization [31]. The membrane reorganization step is usually referred to as pore opening. To understand whether the lag in the cell lysis by HlyII observed at 4 °C is due to the pore opening step, we studied the formation of pore in the presence of osmotic protectants. HlyII (2 HU/ml) was incubated with 1% (v/v) RBC in PBS containing 30 mM PEGs 600 or 1000 for 5 min at different temperatures (4, 25 and 37 °C). The hemolysin was assumed to be bound to the membrane under these conditions because nearly complete hemolysis was observed in the absence of osmotic protectant after the transfer of RBC to the HlyII-free buffer and incubation at 25 °C for

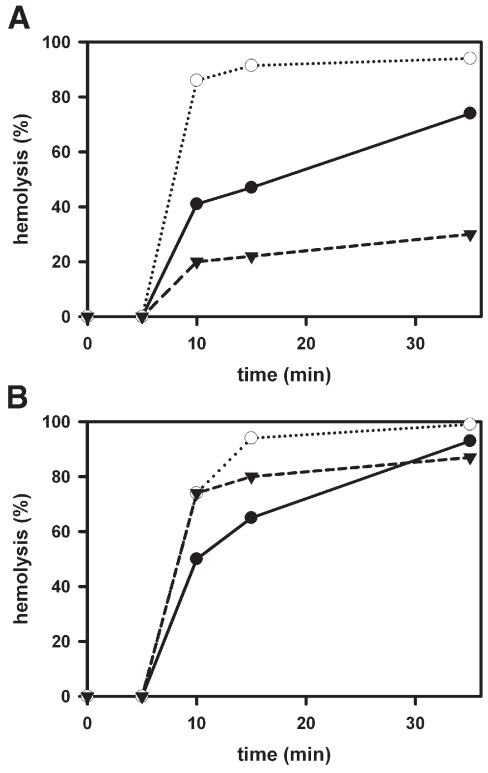

Fig. 4. Effect of temperature on HlyII pore formation. HlyII (8 HU) was mixed with 5 ml of 1% (v/v) human RBC in PBS containing 30 mM PEG 600 (A) and PEG 1000 (B). After incubation at 4 °C (filled circles, solid line), 25 °C (open circles, short dashed line) and 37 °C for 5 min (filled triangles, dashed line), the samples were centrifuged at 1000×*g* for 3 min at 4 °C. The cell pellets were resuspended in 5 ml of PBS (without PEG 600) pre-incubated at 25 °C. The samples were left at this temperature and the time course of hemolysis was followed. Each curve represents the average of three independent experiments. The error bars (not shown) were within the 5% limit of data values.

35 min. Also, the pores could be successfully formed at a low temperature in the presence of non-protective PEGs. Most RBCs remained intact in the presence of PEGs with less than 5% lysis. The samples were then centrifuged at 14,000×*g* for 1 min at 4 °C, and the supernatant was removed. Cell pellets were washed as described above and re-suspended in 1 ml of PBS pre-conditioned at 25 °C. Incubation of the samples was continued at this temperature, and the release of hemoglobin from all samples was recorded after 5, 10 and 30 min. Fig. 4 demonstrates a striking difference between two experiments. After an incubation with PEG 1000 (Fig. 4B), the rate of hemolysis depended on the temperature of pore formation in a way similar to that in our kinetic experiments, i.e., we observed a faster initial rate at a high temperature and the highest overall hemolysis at 25 °C. In the parallel experiments with PEG 600 (Fig. 4A), at 37 °C the hemolysis rate and final yield were lowest, hemolysis never reached 100% and saturated at about 20%. However, complete hemolysis of these samples can be easily obtained by using a detergent or by osmotic shock. The hemolysis at lower temperatures was similar to that observed in the experiments with PEG 1000.

These results may indicate that PEG 600 molecules were capable of permanently staying inside the HlyII lumen if pores were formed at 37 °C and were incapable of doing this when pores were formed at 4 and 25 °C. So, *pore structures vary at different temperatures*. Moreover, the initial temperature of pore formation is crucial for the hemolysis rate and yield: once formed, the pore structure cannot be 'improved'.

3.5. The properties of HlyII ionic channels formed in planar lipid bilayers

Finally, the properties of HlyII pores were examined using the planar lipid bilayer technique. HlyII is capable of opening pores in planar lipid bilayers (Figs. 5 and 6) as is αHL does [32]. Some of HlyII properties, e.g., single channel conductance, shape of the current–voltage (*I–V*) characteristic and ionic selectivity, were investigated. In 100 mM KCl, the pores normally stay open most of the time (Fig. 5A), as do those formed by αHL [33]. Some channel closures are observed only at relatively high voltages. The channel conductance was determined from the height of the current steps upon toxin addition (Fig. 5A and D). The distribution of conductance under these conditions was unusually broad (Fig. 5B), with three peaks corresponding to 18±6, 31±3 and 46±9 pS (30±3 if treated as a single Gaussian). The *three-mode distribution may reflect* alternative paths for ions, which results in different conductances for *different pore structures*. αHL has a different mean conductance in these conditions, 107±3.2 pS [33]. This difference is apparently not related to the pore radii, which are very similar according to the osmotic protection experiments and protein modelling. A higher concentration of charged residues in the HlyII pore lumen is probably responsible for this effect. The *I–V* curve of HlyII open pore was markedly symmetrical and linear within the interval from −100 mV to +100 mV (Fig. 5C) at 100 mM KCl.

The kinetic behavior of the channels did not change when the concentration of KCl was increased up to 1 M (Fig. 5D). The distribution was broad too, with three peaks with the means at 266±80, 502±73 and 805±55 pS, as shown in Fig. 5E. It is worth noting that the properties of the median peak are close to those obtained for gel-eluted HlyII pores formed in detergent [7]. The same results can be fitted by a single normal distribution, with the mean at 342±35. The *I–V* dependence of the channel changed to a super-linear shape at a negative value and was slightly sub-linear at a positive one (Fig. 5F). This change in the shape of the *I–V* curve may reflect additional barriers on the ion route due to the increase of channel hydrophobicity. Additionally, at high salt conditions, we observed that the *I–V* curve had a characteristic N-shape. Usually, this channel property is interpreted as voltage-dependent gating [34].

Thus, we found that, together with most porins and other βPFTs, HlyII exhibits a voltage-induced gating in 1 M KCl at a relatively low voltage starting from −100 mV. This can be confirmed by an additional experiment. When we fix the negative potential at about −100 mV, the channels switch to a special non-ground state with low conductance (Fig. 6). Once the potential was reversed, the value of the initial conductance restored immediately. This experiment demonstrates that the

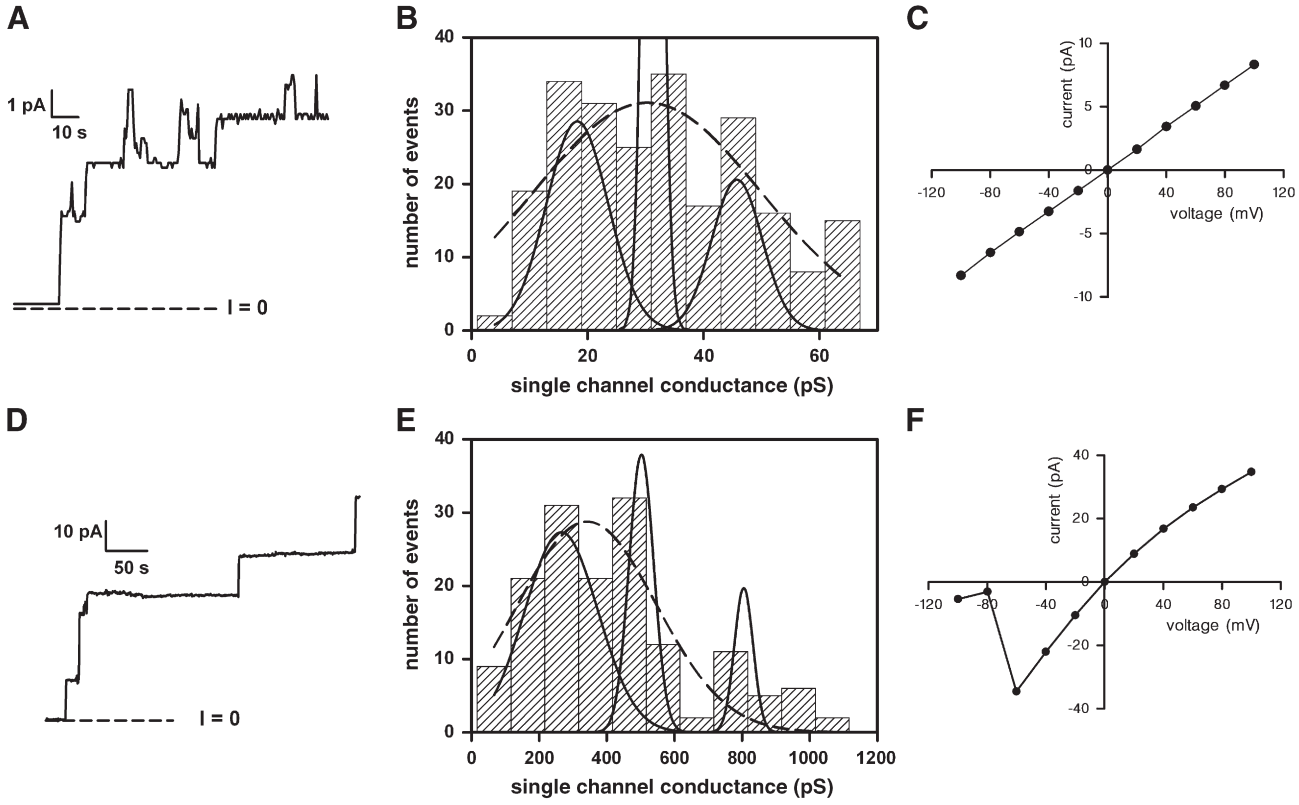

Fig. 5. Electrophysiological properties of HlyII channels. (A, D) The left column illustrates a typical current recording of single channels spontaneously formed by HlyII monomer added to the *cis* compartment (final concentration ~50 ng/ml) containing 100 mM (A) and 1000 mM KCl (D), respectively. (B, E) Conductance histograms of single channels formed by HlyII in 100 mM (B) and 1000 mM KCl (E). The histograms comprise the conductance values of 230 (B) and 150 (E) channel formation events (4–5 channels per membrane). The dashed lines indicate the best fit by a single normal distribution to the most probable conductance values near 30 pS at 100 mM KCl and 342 pS at 1000 mM KCl. The solid lines show an alternative treatment of the results indicating several sub-states by fitting by three separate distributions. All the other conditions for the experiment are described in Materials and methods. (C, F) Steady-state current–voltage relationships of single channels formed by HlyII (C) in 100 mM and 1000 mM (F), respectively. Each *I–V* dataset represents the averages of 3 to 5 independent experiments.

gating observed is reversible, not due to either the loss of protein pore during the procedure or irreversible changes in the pore structure. Under similar conditions, αHL pores do not demonstrate any gating. We make no assumptions as to the physiological relevance of the observed phenomena, as they were observed under non-physiological conditions, and seek merely to understand a distinctive feature of the HlyII pores. Interestingly, an earlier study found no HlyII gating [7]. This difference as well as the differences in the *I–V* dependence can be explained by the nature of the material used in the experiments. In the work referred to, HlyII protein was obtained in a cell-free expression system, eluted from gel as *heptamer* and used under conditions similar to those of this work. We believe that detergent-formed oligomers may represent a uniform population of well-ordered structures, with the prevalence of one of several possible subspecies. Our results may reflect the existing variations in the formation of oligomers with some intermediates or of different stoichiometry. For example, as it was shown in [29], the oligomers formed in deoxycholate micelles migrate as a single band, more slowly than those solubilized from phospholipid vesicles with either deoxycholate or Triton X-100. The different migration rate indicates that the aHL oligomer formed in deoxycholate micelles is slightly larger than that formed in the bilayer, supporting the existence of aHL oligomers of different subunit stoichiometry under these conditions. Also, the published protein sequence [7] contained several unusual amino acid substitutions; all of them were not in the channel interior (Fig. 2

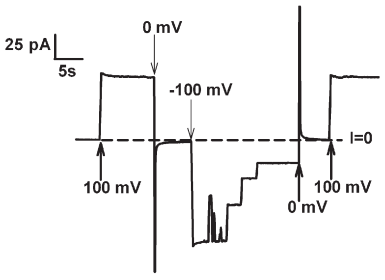

Fig. 6. Current recordings of HlyII toxin channel voltage gating at −100 mV. The voltage gating was observed only in 1000 mM KCl. First, 30 mV was applied to the membrane. After addition of toxin (final concentration 50 ng/ml) we waited for 3–4 single channels to open and then applied voltage pulses. Arrows indicate the sign and value of pulses applied to the membrane. The zero voltage was clamped to standardize the starting conditions. At the fixed positive potentials the channels were in the open state during all the time of the recording. At the negative potentials −60 mV, the spontaneous transition of the channels to the low-conductance level was observed. The data on the figure were taken at −100 mV. Once the positive potentials were applied, the initial conductance values were restored. The dashed line indicates the zero current level.

in Supplement). According to the HlyII pore model, at least three separate belts of charged residues exist in the structure, and pore opening may require conformational changes of all of them. These changes may not be exactly complete, especially at high salt, leading to the partially opened or closed states that can be seen in the planar lipid bilayer system as gating.

The HlyII modified membranes were strongly anion-selective. The selectivity decreased with the ionic strength going up. The reversal potential under salt gradient conditions was measured in a series of experiments. The measurements of the channel selectivity found a reversal potential of −12.2± 0.82 mV in a 3-fold concentration gradient of 0.12/0.04 M and −20.0±0.84 mV in a 5-fold difference of 1.0/0.02 M. The permeability ratio, P_K^+/P_{Cl}^-, for both these gradients was very similar: 0.27 and 0.26, respectively. At higher salt concentrations, 3 M/1 M, the channels had weak anion selectivity: the reversal potential was equal to −2.75±0.75 mV and P_{K+}/P_{Cl-}= 0.46. These data are in complete agreement with [7]. The HlyII pore is significantly more anion-selective than the αHL pore (P_K^+/P_{Cl}^-=0.79, under the same conditions) [35], whereas, e.g., leukocidin pores are cation-selective (P_K^+/P_{Cl}^-=1.64) [7]. Ion selectivity differences should, therefore, be due to the influence of charges that are present in the pore lumen. Inspection of sequence alignments (see Supplement, Figs. 1 and 2) and our model (Fig. 1A–C) indicated interesting differences in the stem region. The lumen of the stem of the αHL pore is neutral because of charge compensation between the residues, i.e., Glu111–Lys147 at its entrance and Asp127–Lys131 at its exit. A similar compensation occurs in HlyII where we can find three pairs of compensated charged residues, but at the pore exit we may see that Lys125 has no immediate charged partner, because Asp124 is directed outside of the pore interior and, probably, contacts the cell contents. So, the overall positive charge in the HlyII pore lumen is likely to contribute to the observed anion selectivity [36].

Taken together, these data are a good illustration of the functional variation of HlyII pores in response to different surroundings during the pore formation and action. The obvious continuation of these experiments, the study of temperature dependence of the interaction of HlyII with lipid bilayers is currently in progress.

4. Discussion

Hemolysin II, together with other members of the β-barrel PFT family, is capable of disrupting the permeability barrier of model and cell membranes, thus leading to the release of vesicle or cell contents. This process, the cell lysis, appears to be the endpoint of a complex series of events.

HlyII is secreted as a 42 kDa water-soluble protein, after removing the signal peptide by the bacterial secretion apparatus [17]. It binds strongly to the membranes to form relatively small pores with an inner diameter of about 1 nm. The sequence homology with staphylococcal toxin is about 30% but the core amino acids are rather conserved. The overall charge of the HlyII protein surface and the lumen interior differs significantly from αHL, which explains the variation in the electrophysiological properties. The exact number of subunits is unknown, but we believe that in ideal experimental conditions HlyII, probably, forms well-shaped homo-heptameric pores [7]; in real life, however, a variety of structures can be observed. The prevalence of the heptameric form is confirmed by our EM study, where most pores appear to be heptameric, and is suggested by the successful homology modeling of the HlyII heptamer structure using the αHL heptamer 3D structure as a template. (It should be noted that αHL structure was obtained by crystallization from the detergent solution. There is no information as to what happens under other conditions.) Our modeling experiments show that there is no interdiction to form an octamer, but hexamer formation is less likely (Supplement, Fig. 5). Broad and tri-modal distribution of channel conductance may also indicate that not all HlyII pores have identical structures. The ratio of conductances obtained (1–1.7–2.6 (in 100 mM KCl) and 1–1.9–3 (in 1000 mM KCl) is in agreement with the possible existence of mix hexamer, heptamer and octamer subspecies assuming that the conductance is proportional to the channel flow area. The predicted ratio obtained using our models of different oligomeric states is 1–1.8–2.5. (To estimate the ratio, we assumed that addition or deletion of one subunit influences neither side chain position nor the other channel properties besides conductance).

The first binding step of HlyII is simple; it binds to the membrane quickly at any temperature we tested. Probably, at low temperatures it associates with the membranes as a monomer, but at higher temperatures as an oligomer of several subunits that pre-exists in protein solutions. The number of subunits in the associates varies, and at high concentrations the oligomers can lead to the deactivation of the toxin. The so-called Arrhenius effect [4] may reflect a partial disruption of the associates heated at moderate temperatures. The specific activity of HlyII is higher than that of αHL. Also, according to Miles et al. [7], the initial lag period associated with HlyII hemolysis is relatively short compared with αHL: HlyII, 5 min to 50% lysis at HC50; αHL, 18 min to 50% lysis at HC50. HlyII interacts with naked artificial membranes and different types of mammal cells equally well [17].

The binding of the monomer to the membrane is followed by oligomerization. Obviously, this stage is cooperative. Little is known either about this process or its kinetics or else about the conformational changes the protein subunits undergo. As the result of oligomerization, a pre-pore is probably formed. According to our data, its structure is temperature-dependent. It seems that at high temperature the transition from a narrower state to a wider fully open pore is rapid, or no intermediates exist at all. We believe that, depending on temperature, concentration of monomer and, probably, type of membrane, the mechanism of pore formation by hemolysin II can differ; both the pre-pore and growing pore models can be used to describe it [31].

The properties of HlyII pores were studied. We were able to obtain EM images of the HlyII pores formed in artificial membranes. It seems that their structures are slightly different from the image we obtained as the result of structural modeling. The real pores are rounder in shape and less symmetrical. These

differences can be explained by the absence of a C-terminal domain in the model, which can possibly provide additional interactions between the subunits. It should be noted that the C-terminal part is absent in αHL [12] and has no significant sequence similarity with any protein in the database. We suggest that HlyII C-terminus exists as an independent protein domain based on its sensitivity to proteolytic digestion. Also, HlyII lacking the C-terminus domain retains a hemolytic activity and a capability of forming pores [7]. The results of C-term *de novo* protein modeling are shown in Supplement, Fig. 7. Exact position and orientation of the domain cannot be predicted by modern bioinformatic means but it seems to be structured and cannot block the pore entrance. Another explanation is that the conditions of pore formation were not perfect: we did not pre-form oligomers in detergent solution before their insertion in the liposome membrane but allowed them to be formed spontaneously. The differences in the pore properties obtained at different temperatures are surprising. Whether these differences reflect the changes in the distribution of different oligomeric forms or not is an open question and should be tested experimentally. Gating of the pores we observed under specific conditions is an intriguing property. The role of some charged residues (including E141) in this phenomenon is under investigation and will be published somewhere.

Acknowledgments

We thank Oleg Kovalevskiy and Vasili Hauryliuk for critical reading of the manuscript, and Laboratory of Bioinformatics and Protein Engineering, International Institute of Molecular and Cell Biology, Warsaw, Poland for their help with 3D homology modeling. We also thank Victor Selivanov for his time and effort in copyediting the paper.

Appendix A. Supplementary data

Supplementary data associated with this article can be found, in the online version, at doi:10.1016/j.bbamem.2006.11.004.

References

[1] F.A. Drobniewski, *Bacillus cereus* and related species, Clin. Microbiol. Rev. 6 (1993) 324–338.
[2] P.E. Granum, *Bacillus cereus*, Fundamentals in Food Microbiology, ASM, Washington, DC, 1997, pp. 327–336.
[3] B. Promdonkoy, D.J. Ellar, Investigation of the pore-forming mechanism of a cytolytic delta-endotoxin from *Bacillus thuringiensis*, Biochem. J. 374 (2003) 255–259.
[4] M.A. Sinev, Z. Budarina, I.V. Gavrilenko, A.I. Tomashevskii, N.P. Kuz'min, Evidence of the existence of hemolysin II from *Bacillus cereus*: cloning the genetic determinant of hemolysin, Mol. Biol. (Moscow) 27 (1993) 1218–1229.
[5] Z.I. Budarina, M.A. Sinev, S.G. Mayorov, A.Y. Tomashevski, I.V. Shmelev, N.P. Kuzmin, Hemolysin II is more characteristic of *Bacillus thuringiensis* than *Bacillus cereus*, Arch. Microbiol. 161 (1994) 252–257.
[6] G.E. Baida, N.P. Kuzmin, Mechanism of action of hemolysin III from *Bacillus cereus*, Biochim. Biophys. Acta 1284 (1996) 122–124.
[7] G. Miles, H. Bayley, S. Cheley, Properties of *Bacillus cereus* hemolysin II: a heptameric transmembrane pore, Protein Sci. 11 (2002) 1813–1824.
[8] E. Gouaux, M. Hobaugh, L. Song, Alpha-hemolysin, gamma-hemolysin, and leukocidin from *Staphylococcus aureus*: distant in sequence but similar in structure, Protein Sci. 6 (1997) 2631–2635.
[9] E. Gouaux, alpha-Hemolysin from *Staphylococcus aureus*: an archetype of beta-barrel, channel-forming toxins, J. Struct. Biol. 121 (1998) 110–122.
[10] T. Lund, M.L. De Buyser, P.E. Granum, A new cytotoxin from *Bacillus cereus* that may cause necrotic enteritis, Mol. Microbiol. 38 (2000) 254–261.
[11] A. Fagerlund, O. Ween, T. Lund, S.P. Hardy, P.E. Granum, Genetic and functional analysis of the cytK family of genes in *Bacillus cereus*, Microbiology 150 (2004) 2689–2697.
[12] L. Song, M.R. Hobaugh, C. Shustak, S. Cheley, H. Bayley, J.E. Gouaux, Structure of staphylococcal alpha-hemolysin, a heptameric transmembrane pore, Science 274 (1996) 1859–1865.
[13] N.C. Caiazza, G.A. O'Toole, Alpha-toxin is required for biofilm formation by *Staphylococcus aureus*, J. Bacteriol. 185 (2003) 3214–3217.
[14] V. Noireaux, A. Libchaber, A vesicle bioreactor as a step toward an artificial cell assembly, Proc. Natl. Acad. Sci. U. S. A. 101 (2004) 17669–17674.
[15] G. Menestrina, M. Dalla Serra, G. Prevost, Mode of action of beta-barrel pore-forming toxins of the staphylococcal alpha-hemolysin family, Toxicon 39 (2001) 1661–1672.
[16] Z.I. Budarina, D.V. Nikitin, N. Zenkin, M. Zakharova, E. Semenova, M.G. Shlyapnikov, E.A. Rodikova, S. Masyukova, O. Ogarkov, G.E. Baida, A.S. Solonin, K. Severinov, A new *Bacillus cereus* DNA-binding protein, HlyIIR, negatively regulates expression of *B. cereus* haemolysin, Microbiology 150 (2004) 3691–3701.
[17] Z.I. Andreeva, V.F. Nesterenko, I.S. Yurkov, Z.I. Budarina, E.V. Sineva, A.S. Solonin, Purification and cytotoxic properties of *Bacillus cereus* hemolysin, Protein Expression Purif. 47 (2006) 186–193.
[18] B. Wallner, A. Elofsson, All are not equal: a benchmark of different homology modeling programs, Protein Sci. 14 (2005) 1315–1327.
[19] R.C. Edgar, MUSCLE: multiple sequence alignment with high accuracy and high throughput, Nucleic Acids Res. 32 (2004) 1792–1797.
[20] S.F. Altschul, T.L. Madden, A.A. Schaffer, J. Zhang, Z. Zhang, W. Miller, D.J. Lipman, Gapped BLAST and PSI-BLAST: a new generation of protein database search programs, Nucleic Acids Res. 25 (1997) 3389–3402.
[21] D. Eisenberg, R. Luthy, J.U. Bowie, VERIFY3D: assessment of protein models with three-dimensional profiles, Methods Enzymol. 277 (1997) 396–404.
[22] M.M. Bradford, A rapid and sensitive method for the quantitation of microgram quantities of protein utilizing the principle of protein-dye binding, Anal. Biochem. 72 (1976) 248–254.
[23] R. Scherrer, B.T. Cabrera, P. Gerhardt, Macromolecular sieving by the dormant spore of *Bacillus cereus*, J. Bacteriol. 108 (1971) 868–873.
[24] P. Mueller, D.O. Rudin, Induced excitability in reconstituted cell membrane structure, J. Theor. Biol. 4 (1963) 268–280.
[25] B. Hille, Ionic Channels of Excitable Membranes, Sinauer Associate Publishers, Sunderland, MA, 1984.
[26] A. Aksimentiev, K. Schulten, Imaging alpha-hemolysin with molecular dynamics: ionic conductance, osmotic permeability, and the electrostatic potential map, Biophys. J. 88 (2005) 3745–3761.
[27] A. Yu Bakulina, E.V. Sineva, A.S. Solonin, A.Z. Maksyutov, Molecular modeling of *B. cereus* hemolysin II, a pore-forming protein, Proc. 5th Int. Conf. on Bioinformatics of Genome Regulation and Structure (BGRS'2006), Novosibirsk, Russia, July 16–22, 2006, 2006, pp. 231–234, http://www.bionet.nsc.ru/meeting/bgrs2006/.
[28] G. Viero, R. Cunaccia, G. Prevost, S. Werner, H. Monteil, D. Keller, O. Joubert, G. Menestrina, M. Dalla Serra, Homologous versus heterologous interactions in the bicomponent staphylococcal gamma-haemolysin pore, Biochem. J. 394 (2006) 217–225.
[29] D.M. Czajkowsky, S.T. Sheng, Z.F. Shao, Staphylococcal alpha-hemolysin can form hexamers in phospholipid bilayers, J. Mol. Biol. 276 (1998) 325–330.
[30] R.Z. Sabirov, Y. Okada, Wide nanoscopic pore of maxi-anion channel suits its function as an ATP-conductive pathway, Biophys. J. 87 (2004) 1672–1685.
[31] S.J. Tilley, E.V. Orlova, R.J. Gilbert, P.W. Andrew, H.R. Saibil, Structural

basis of pore formation by the bacterial toxin pneumolysin, Cell 121 (2005) 247–256.
[32] G. Menestrina, Ionic channels formed by *Staphylococcus aureus* alpha-toxin: voltage-dependent inhibition by divalent and trivalent cations, J. Membr. Biol. 90 (1986) 177–190.
[33] P.G. Merzlyak, L.N. Yuldasheva, C.G. Rodrigues, C.M. Carneiro, O.V. Krasilnikov, S.M. Bezrukov, Polymeric nonelectrolytes to probe pore geometry: application to the alpha-toxin transmembrane channel, Biophys. J. 77 (1999) 3023–3033.
[34] G. Bainbridge, I. Gokce, J.H. Lakey, Voltage gating is a fundamental feature of porin and toxin beta-barrel membrane channels, FEBS Lett. 431 (1998) 305–308.
[35] L.Q. Gu, S.M. Dalla, J.B. Vincent, G. Vigh, S. Cheley, O. Braha, H. Bayley, Reversal of charge selectivity in transmembrane protein pores by using noncovalent molecular adapters, Proc. Natl. Acad. Sci. U. S. A. 97 (2000) 3959–3964.
[36] Y.E. Korchev, G.M. Alder, A. Bakhramov, C.L. Bashford, B.S. Joomun, E.V. Sviderskaya, P.N. Usherwood, C.A. Pasternak, *Staphylococcus aureus* alpha-toxin-induced pores: channel-like behavior in lipid bilayers and patch clamped cells, J. Membr. Biol. 143 (1995) 143–151.